

**REAL-TIME TRACKING OF LINAC
PARAMETERS FOR VERIFICATION OF DYNAMIC
MULTILEAF COLLIMATOR (DMLC) BASED
RADIOTHERAPY TREATMENT**

NUR SHAHEERA BINTI MIDI

UNIVERSITI SAINS MALAYSIA

2018

**REAL-TIME TRACKING OF LINAC
PARAMETERS FOR VERIFICATION OF DYNAMIC
MULTILEAF COLLIMATOR (DMLC) BASED
RADIOTHERAPY TREATMENT**

by

NUR SHAHEERA BINTI MIDI

**Thesis submitted in fulfilment of the requirement
for the degree of
Master of Science**

July 2018

ACKNOWLEDGEMENT

For this project to be completed special thanks to my supervisor, Dr Mohd Hafiz Mohd Zin for his constant guidance throughout the project. I also want to thank the staff in Radiotherapy Unit, Advanced Medical and Dental Institute for their cooperation in completing the project. A credit also goes to Mr Koh K.L (Abex Medical System). Mr Lim Lih Chee (Loh Guan Lye Specialist Hospital), Mr Chin Le Fei and Miss Nurfaizra Shafiee for their help in the preliminary work of the study. Special thanks also for my friends and family for their encouragement in completing this project.

TABLES OF CONTENT

ACKNOWLEDGEMENT	II
TABLES OF CONTENT	III
LIST OF TABLES	V
LIST OF FIGURES	VI
LIST OF ABBREVIATIONS	IX
ABSTRAK	XI
ABSTRACT	XII
CHAPTER 1 INTRODUCTION	1
1.1 Introduction to radiotherapy	1
1.2 Linear accelerator for modern radiotherapy	3
1.2.1 Linear accelerator (linac)	3
1.2.2 Dynamic multileaf collimator (dMLC)	6
1.3 Dynamic MLC based radiotherapy treatment	8
1.3.1 Intensity Modulated Radiation Therapy (IMRT)	9
1.4 Quality assurance of IMRT and VMAT using clinical detectors	11
1.5 Real-time tracking data of linac parameters	13
1.5.1 Varian linac	13
1.5.2 Elekta linac	16
1.6 Purpose of study	18
CHAPTER 2 MATERIALS AND METHODS	19
2.1 Varian Clinac iX	19
2.1.1 Varian Millennium 120 MLC and tracking system	19
2.1.2 Characterisation of real-time tracking data from Varian linac	19
2.1.2(a) Varian log file	19
2.1.3 Application of real-time data tracking on clinical IMRT plan for treatment verification	23
2.2 Elekta Synergy	27
2.2.1 Elekta Agility 160 MLC and the tracking system	27
2.2.2 Characterisation of real-time tracking data from Elekta linac	28
2.2.2(a) Static field	28
2.2.2(b) Dynamic MLC and dynamic Arc plan	33
2.2.3 Application of real-time data tracking on clinical IMRT plan for treatment verification.	36

CHAPTER 3	RESULTS	38
3.1	Varian Clinac iX	38
3.1.1	Characteristics of real-time tracking data from Varian linac	38
3.1.2	Application of real-time data tracking on clinical IMRT plan for treatment verification	43
	3.1.2(a) MLC error	43
	3.1.2(b) MLC speed	47
	3.1.2(c) MLC error evaluation on speeds and gantry angle.	49
	3.1.2(d) Fluence map	52
3.2	Elekta Synergy	61
3.2.1	Characterisation of real-time tracking data from Elekta linac	61
	3.2.1(a) Static field	61
	3.2.1(b) Dynamic MLC and dynamic arc plan	65
	3.2.1(c) MLC error evaluation	73
3.2.2	Application of real-time data tracking on clinical IMRT plan for treatment verification	76
	3.2.3(a) MLC error during beam hold-off	76
	3.2.3(b) MLC error during beam-on	81
	3.2.3(c) MLC speed	84
	3.2.3(d) MLC error evaluation as function of MLC speed and gantry angle	86
	3.2.3(e) Fluence map	90
CHAPTER 4	DISCUSSION	99
4.1	Real-time tracking data in patient specific quality assurance	99
4.2	Development of a Graphical User Interface (GUI) of the algorithm for IMRT treatment verification	104
CHAPTER 5	SUMMARY AND CONCLUSION	109
5.1	Summary of results	109
5.2	Future work	113
LIST OF PUBLICATION		115
REFERENCES		116

LIST OF TABLES

		Page
Table 1.0	Mechanical characteristic of Varian Millennium and Elekta Agility MLC system	8
Table 2.1	There IMRT cases delivered using Varian Clinac iX analyses in this study	23
Table 2.2	Tracked linac parameters by service graphing tool	30
Table 2.3	Prescription range of delivery parameters for dArc beam delivery	35
Table 3.1	MLC position error, MLC speed and MLC speed error of analysed IMRT	44
Table 3.2	MLC speed and MLC speed error of analysed IMRT	48
Table 3.3	Gamma pass rate of VLF fluence map	57
Table 3.4	Delivery parameters logged by SG tool	62
Table 3.5	Delivery parameters errors calculated from ELF	62
Table 3.6	Deviation range of delivery parameters in dMLC	69
Table 3.7	Reproducibility of MLC error for dMLC beam.	69
Table 3.8	Deviation range of delivery parameters in dArc	69
Table 3.9	MLC error during treatment delivery including during beam hold off	77
Table 3.10	MLC position error, MLC speed and MLC speed error of analysed IMRT	81
Table 3.11	The IMRT MLC speeds and the RMS MLC speed error	84
Table 3.12	Gamma analysis pass rates and maximum dose deviation for each IMRT cases	88

LIST OF FIGURES

		Page
Figure 1.1	CT image of head and the tumour is shown by the arrow	2
Figure 1.2	Schematic diagram of tumour treatment volume defined by ICRU Report 62	3
Figure 1.3	Linear accelerator from Elekta linac	5
Figure 1.4	Schematic diagram of the linac gantry head	5
Figure 1.5	Photograph of the multileaf collimator	7
Figure 1.6	The sMLC (a) and the dMLC (b) field shape segment delivery (in colour) and the resulted fluence map (in grayscale)	10
Figure 1.7	Optical tracking mechanism for Elekta Agility	16
Figure 2.1	Structure of (a) the VLF data and (b) the data after it was rearranged in Excel	21
Figure 2.2	Flow chart of VLF file extraction algorithm	22
Figure 2.3	Flow chart of fluence map construction algorithm	26
Figure 2.4	Service graphing tool in Elekta linac service mode control system	27
Figure 2.5	The test object for a static square field of 5 cm × 5 cm.	29
Figure 2.6	Trigger function set up in SG tool	29
Figure 2.7	ELF raw file structure	31
Figure 2.8	Extracted delivery parameters from ELF	31
Figure 2.9	Flow chart of ELF extraction algorithm	33
Figure 2.10	CCTV camera to observe the beam light from the linac	35
Figure 3.1	Tracked and prescribed MLC position for (a) Bank A and (b) Bank B at t=12.3 s during IMRT HN 1 treatment delivered at 180° gantry angle	41
Figure 3.2	Tracked and prescribed MLC position for (a) Bank A and (b) Bank B at t=11 s during IMRT HN 1 treatment delivered at 180° gantry angle	42
Figure 3.3	Tracked and prescribed MLC position for (a) Bank A and (b) Bank B at t=13.7 s during IMRT HN 1 treatment delivered at 180° gantry angle	43
Figure 3.4	MLC error count in (a) HN 1 (b) HN 2 and (c) HN 3	46
Figure 3.5	Mean of RMS error for each MLC in HN 1	47
Figure 3.6	Mean of RMS error for each MLC in HN 2	47
Figure 3.7	Mean of RMS error for each MLC in HN 3	48
Figure 3.8	Correlation of control point spacing and MLC speed	49
Figure 3.9	Histogram of MLC speed of HN 3	50
Figure 3.10	MLC error and MLC speed of MLC 21 (Gantry angle 80°) of HN 3. The spike shows the highest MLC speed and the highest MLC error	51

Figure 3.11	MLC error at different MLC speed range for (a) HN 1 (b) HN 2 and (c) HN 3	52
Figure 3.12	MLC error at different gantry angle	53
Figure 3.13	(a) Tracked (b) prescribed and (c) error fluence map of HN 1	55
Figure 3.14	(a) Tracked (b) prescribed and (c) error fluence map of HN 2	56
Figure 3.15	(a) Tracked (b) prescribed and (c) error fluence map of HN 3	57
Figure 3.16	Direction of MLC movement	58
Figure 3.17	Profile of pixel value (a) perpendicular and (b) parallel to MLC movement for HN 1	59
Figure 3.18	Profile of pixel value (a) perpendicular and (b) parallel to MLC movement for HN 2	69
Figure 3.19	Profile of pixel value (a) perpendicular and (b) parallel to MLC movement for HN 3	61
Figure 3.20	Static field from (a) Real-time tracked data (ELF) (b) Film strips for 5 cm x 5 cm square field	64
Figure 3.21	Static field from (a) Real-time tracked data (ELF) (b) Film strips for 10 cm x 10 cm square field	65
Figure 3.22	Tracked MLC position at t (a) 2.75 s (b) 8.25 s during the dMLC delivery	67
Figure 3.23	Tracked MLC position at t (a) 18.5 s and (b) 28.75 s during the dMLC delivery.	68
Figure 3.24	Tracked MLC position at t = 39 s during the dMLC delivery	69
Figure 3.25	MLC position tracked and prescribed for MLC 40 during the entire dMLC beam delivery	69
Figure 3.26	MLC position at (a) t = 0.25 s and (b) t = 8.25 s during dArc delivery	72
Figure 3.27	MLC position at (a) t = 10.5 s and (b) t = 9.5 s during dArc delivery.	72
Figure 3.28	MLC position at (a) t = 13.25 s and (b) t = 45.25 s during dArc delivery	73
Figure 3.29	MLC position error at different speed for MLC 40 (a) during sMLC treatment (b) during dArc treatment	75
Figure 3.30	MLC position error at different (a) gantry angle and (b) gantry speed for MLC 40 in dArc delivery	76
Figure 3.31	Maximum MLC error and beam state for HN 1	79
Figure 3.32	Maximum MLC error and beam state for HN 2	79
Figure 3.33	Maximum MLC error and beam state for HN 3	80
Figure 3.34	Plot of MLC error and prescribed CP spacing for MLC 19, Y1	80
Figure 3.35	MLC error count during beam hold-off for (a) HN 1 (b) HN 2 and (c) HN 3	81

Figure 3.36	MLC error count (a) HN 1 (b) HN 2 and (c) HN 3	83
Figure 3.37	Mean of RMS error for individual MLC for (a) HN 1 (b) HN 2 and (c) HN 3	84
Figure 3.38	MLC speed causes high MLC error (MLC 29 HN 2)	85
Figure 3.39	Histogram of MLC speed of HN 2	86
Figure 3.40	Correlation of MLC speed and prescribed control points spacing	87
Figure 3.41	MLC error at different MLC speed range for (a) HN 1 (b) HN 2 and (c) HN 3	89
Figure 3.42	MLC position error at different speed for right bank MLC 40 (a) HN 1, (b) HN 2, (c) HN 3	90
Figure 3.43	MLC error at different gantry angle	91
Figure 3.44	(a) Tracked, (b) prescribed and (c) error fluence map of HN 1	94
Figure 3.45	(a) Tracked, (b) prescribed and (c) error fluence map of HN 2	95
Figure 3.46	(a) Tracked, (b) prescribed and (c) error fluence map of HN 3	96
Figure 3.47	Profile of pixel value (a) perpendicular and (b) parallel to MLC movement HN 1 at the centre region of fluence map	97
Figure 3.48	Profile of pixel value (a) perpendicular and (b) parallel to MLC movement of HN 2 at the centre region of fluence map	98
Figure 3.49	Profile of pixel value (a) perpendicular 1 and (b) parallel to MLC movement of HN 3 at the centre region of fluence map	99
Figure 3.50	Workflow of IMRT and the GUI developed to analysed the delivery performance	107
Figure 3.51	Main interface of IMRT QA. (a) Summary of MLC error and MLC speeds (b) MLC and fluence analysis GUI	107
Figure 3.52	MLC analysis in the QA software (a) MLC plot (b) MLC error and (c) MLC RMS error	108
Figure 3.53	Tracking fluence map analysis	109

LIST OF ABBREVIATIONS

2D	two-dimensional
3D	three-dimensional
AAPM	American Association of Physicist in Medicine
CT	computed tomography
csv	comma separated value
CTV	clinical target volume
dMLC	dynamic MLC
DTA	distance to agreement
dArc	dynamic arc
EPID	electronic portal imaging device
ELF	Elekta Log File
GUI	Graphical User Interface
GTV	gross tumour volume
HN	head and neck
ICRU	International Commission on Radiation Unit and Measurements
ITV	internal target volume
IMRT	Intensity Modulated Radiation Therapy
MRI	magnetic resonance imaging
MLC	multileaf collimator
MU	monitor unit
PET	positron emission tomography
PTV	planning target volume
QA	quality assurance
RMS	root mean square
sMLC	static MLC
SSD	source to surface distance

SG	service graphing
TG	Task Guide
TPS	treatment planning system
VMAT	Volumetric Modulated Arc Therapy
VLF	Varian Log File

**PENGESANAN MASA NYATA PARAMETER PEMECUT LINEAR UNTUK
VERIFIKASI RAWATAN RADIOTERAPI BERASASKAN KOLIMAT
PELBAGAI LAPISAN DINAMIK (DMLC)**

ABSTRAK

Radioterapi Modulasi Keamatan (IMRT) menyampaikan dos yang konformal kepada tumor menggunakan kolimat pelbagai lapisan dinamik (MLC). Kerumitan IMRT memerlukan pengesanan pra-rawatan khusus pesakit. Kajian ini menyiasat penggunaan data yang dilog pada masa nyata untuk pengesanan rawatan IMRT dari dua pemecut linear radioterapi moden bagi mekanisma pengesanan yang berbeza. Pemecut linear Varian menggunakan mekanisma arus motor untuk mengesan MLC dan data dilog sebagai Varian log file (VLF), manakala pemecut linear Elekta menggunakan sistem pengesan optik dan data dilog sebagai Elekta Log File (ELF). Data yang dijejak daripada tiga rawatan IMRT kes kepala dan leher (HN) dari kedua-dua jenis pemecut linear dianalisis menggunakan algoritma yang dibangunkan menggunakan Matlab (Mathworks, Natick, MA). Struktur data daripada VLF yang dianalisis berpadanan dengan literatur. Algoritma untuk ELF juga dicipta berdasarkan algoritma VLF. Ia digunakan untuk menilai ketepatan pelan IMRT dan menganalisis prestasi MLC IMRT yang dilakukan pemecut linear. Analisis rawatan IMRT yang dilog VLF menunjukkan bahawa ralat kedudukan MLC semasa rawatan adalah antara -1.3 hingga 2.1 mm. Ralat kedudukan MLC untuk rawatan IMRT dilog ELF adalah lebih tinggi antara -3.0 hingga 3.9 mm. Walaubagaimanapun, hanya 1% daripada ralat tersebut melebihi nilai rekomendasi 3.5 mm oleh AAPM TG 142. Perbezaan parameter lain yang dikesan juga dalam toleransi. Peratusan kadar lulus indeks gama adalah antara 97.46% hingga 99.76% untuk VLF dan 97.45% kepada 100% untuk ELF. Aplikasi pengesan masa nyata adalah berguna dalam pengesanan rawatan radioterapi dan penilaian prestasi MLC.

**REAL-TIME TRACKING OF LINAC PARAMETERS FOR VERIFICATION
OF DYNAMIC MULTILEAF COLLIMATOR (DMLC) BASED
RADIOTHERAPY TREATMENT**

ABSTRACT

Intensity Modulated Radiation Therapy (IMRT) delivers highly conformal dose to tumour using dynamic multileaf collimator (MLC). The complexity of IMRT delivery requires patient specific pre-treatment verification. This study investigates application of real-time tracking data for IMRT verification from two modern radiotherapy linacs of different tracking mechanism. Varian linac uses motor current feedback to track the MLC and logged the data as Varian log file (VLF), whereas Elekta linac uses optical tracking system and logged the data as Elekta log file (ELF). The tracking data from three head and neck (HN) IMRT treatments from both linacs were analysed using algorithms developed with Matlab (MathWorks, Natick, MA). The data structure of the VLF analysed agrees with the literatures. Another algorithm was developed to characterise ELF, based on the VLF algorithm developed. The algorithm was used to evaluate the accuracy of the IMRT plans and the MLC performance delivered from the linac. Analysis of IMRT delivery logged in VLF shows that the MLC error during treatment is between -1.3 to 2.1 mm. The MLC error for IMRT delivery logged in ELF is higher between -3.0 to 3.9 mm. However, only 1% of the error is above the AAPM TG 142 recommended 3.5 mm tolerance value. The discrepancies of other tracked treatment parameters are also within the tolerance. Percentage gamma pass rates of IMRT delivery ranges from 97.46% to 99.76% for VLF and 97.45% to 100% for ELF. Real-time tracking data is useful for verification of dMLC based radiotherapy delivery and evaluation of the MLC performance.

CHAPTER 1 INTRODUCTION

1.1 Introduction to radiotherapy

Cancer is a disease triggered by the uncontrolled growth of abnormal cells in a tissue that could spread to other parts of the body. Treatment of cancer may involve surgery, chemotherapy, radiotherapy or combination of the techniques. Radiotherapy utilises ionising radiation to deliver lethal dose to the cancerous tumour target while sparing normal tissue structure.

Radiotherapy treatment includes several stages. After cancer diagnosis, the first stage of radiotherapy is the treatment planning process involving the localisation of the tumour. The patient position is fixed using immobilisation device such as thermoplastic mask. Images of the tumour position are acquired using computed tomography (CT) scanner and in some cases in combination with other imaging modalities such as magnetic resonance imaging (MRI) and positron emission tomography (PET). These imaging modalities provide 3 dimensional (3D) anatomical information of the patient [1]. Figure 1.1 shows an example of an image of a tumour in the head region scanned using CT scanner. The image provides information of the tumour location that should receive the optimal dose and the surrounding normal tissue that should be spared.

An oncologist will outline the tumour regions that need to be treated and determine the total radiation dose to be delivered during treatment planning. Tumour delineation follows the recommendation by the International Commission on Radiation Unit and Measurements (ICRU). Figure 1.2 is a schematic representation of tumour volumes in radiotherapy defined by ICRU Report 62 [2]. Gross tumour volume (GTV) is the distinguishable location of the tumour that is determined by the visible

tumour region in the image. It consists of the position and the extend of the primary tumour. Clinical target volume (CTV) is the volume that surrounds the GTV. It is an extension of microscopic tumour spread which has to be eliminated alongside the primary tumour. Internal target volume (ITV) represents the uncertainties of CTV due to movement. It is likely to include the internal organ motion. To ensure the prescribed dose is delivered to the CTV, planning target volume (PTV) is defined. PTV accommodates the net effect of all possible geometrical variations and inaccuracies.

The next processes are the dose calculation and beam arrangement that are performed using computerised treatment planning system by the physicist or dosimetrist. This process determines the radiotherapy delivery technique, fractional dose and the treatment field parameters. The final treatment plan will be evaluated to achieve the treatment prescription. The treatment plan contains the information on the treatment delivery parameter such as the total dose, fractional dose and collimator positions. A final verification of the treatment plan is required to ensure that each of the planned treatment beam and dose delivered covers the tumour of the target volume and the critical normal tissues are spared.



Figure 1.1: CT image of head and the tumour is shown by the arrow [3]

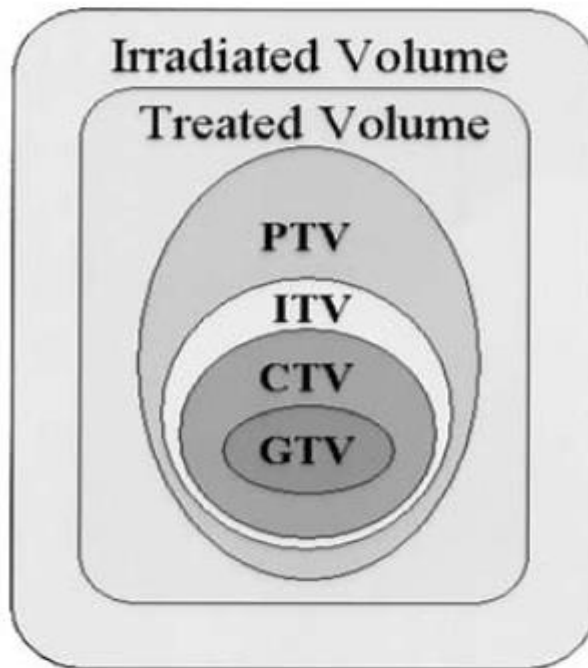


Figure 1.2: Schematic diagram of tumour treatment volume defined by ICRU Report 62

1.2 Linear accelerator for modern radiotherapy

1.2.1 Linear accelerator (linac)

Radiotherapy uses a linac to produce high energy radiation beam and conform the beam to the planned target. A linac consists of a rotating gantry head and treatment couch (Figure 1.3). Figure 1.4 shows the schematic diagram of the gantry head where the high energy radiation beam production takes place. Linac uses high frequency electromagnetic waves to accelerate electrons to a speed approaching speed of light in a linear vacuum tube called waveguide. A magnetron controls the power and frequency of the electromagnetic waves, in which later determines the energy of the x-ray produced.

Electrons are produced from an electron gun (cathode) situated at the end of the waveguide, by heating the tungsten filament within the cathode. The number of electrons ejected are controlled by the temperature of the filament. The electrons are injected to the waveguide and accelerates along it. As the electron beam exits the waveguide it enters a flight tube which contains bending magnet that will bend the electron beam towards the target. The high energy electron beam hits the target and the interaction produces photons. High energy photons emerge from the target in a variety of directions. It will then pass through a primary collimator. Primary collimator only allows photons that are travelling in a forward direction to pass through it thus producing a cone shaped beam. The photons are still not uniformly distributed across the beam, so a flattening filter is placed in the path of the photons. The filter absorbs more photons at the centre thus producing a more uniform beam.

Two ion chambers are located below the filter for dose monitoring. One of the ion chamber acts as a primary dosimeter. It measures the radiation dose and the beam quality such as the symmetry and flatness of the beam. The ion chamber stops the beam delivery when the required doses have been delivered or the beam quality is outside the acceptance level. The secondary chamber acts as a backup when the primary dosimeter failed to function.

The photon beam is shaped using a collimator to deliver a beam that is more conformal to the tumour. Conventional beam shaping was done using sets of dense metal collimator called the “jaws” to produce a rectangular or square field. A secondary beam blocks that comes with a range of shapes and sizes needed to be attached manually to the jaws to create an irregular beam shape. The drawback of this conventional method is that it only allows limited number of beam shape that will restrict the conformity of the beam [4]. Furthermore the use of blocks were inefficient

as they are time-consuming to be produced and are made up of cerrobend, a toxic material [4]. A more flexible beam shaping system uses the multileaf collimators (MLC). The specification of the multileaf collimator will be further discussed in Section 1.2.2.

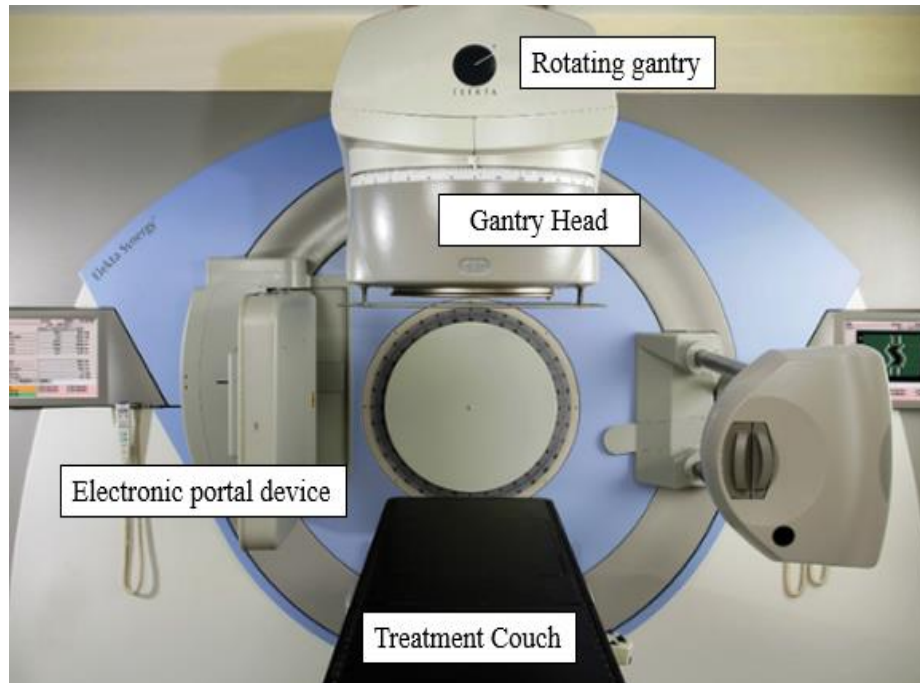


Figure 1.3 Linear accelerator from Elekta linac (www.oncologysystems.com).

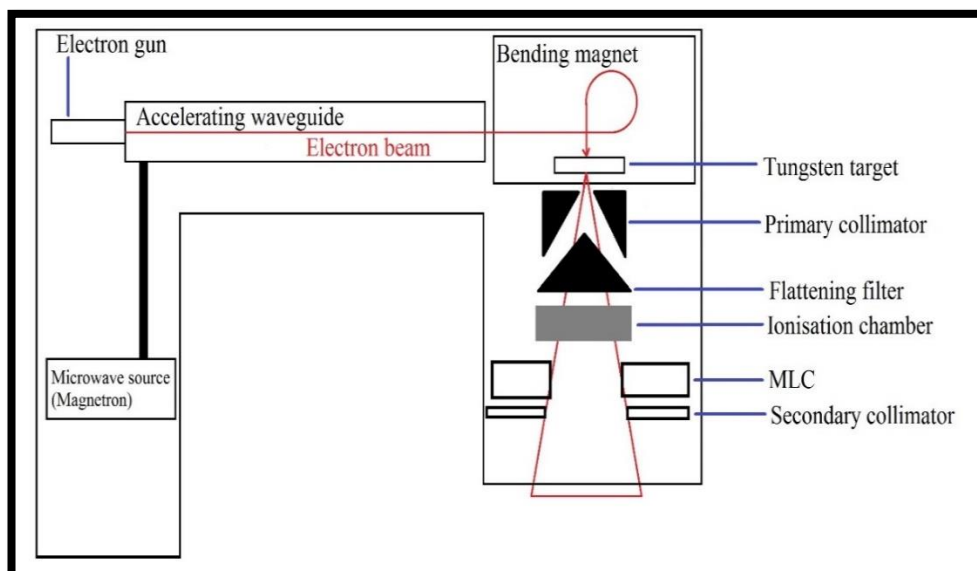


Figure 1.4: Schematic diagram of the linac gantry head.

1.2.2 Dynamic multileaf collimator (dMLC)

Multileaf collimator (MLC) consists of pairs of individual leaf blades in which each leaf moves independently to create a variety of complex treatment shapes. MLCs are motorised leaves arranged in two opposing rows as shown in Figure 1.5. Each of them moves independently from each other. MLCs can either move in sequence of fixed position during beam off (step-and-shoot MLC) or continuously to move while the beam on (dynamic MLC) [5]. The movement allows the creation of a more complex beam shape to modulate the beam intensity of the treatment field. Automated field shaping by the MLC increases the conformality of the beam and reduces radiotherapist workload compared to the conventional method.

MLCs are made of tungsten, a high density material with low thermal expansion [4]. Table 1 shows the technical characteristic of two commercial MLC systems, Varian Millennium (Varian Medical System, Palo Alto, USA) [4] and Elekta Agility (Elekta, Crawley, UK) [6] that were used in this study.

Varian Millennium linac MLC system consists of 120 MLCs. They are arranged in two MLC banks, each consists of 60 MLCs. From the beam eye's view, the right and left MLC bank is known as Bank A and Bank B respectively. 20 outer leaf pairs are 1.0 cm in width while 40 middle leaf pairs are 0.5 cm in width. MLCs are numbered from 1 until 60 from the positive Cartesian coordinate from the beam eye's view. This arrangement of leaves allows the production of 40 x 40 cm² maximum field size. The maximum MLC speed is 2.5 cm/s.

Elekta Agility linac consists of 160 MLCs. They are arranged to two MLC banks, each bank consist of 80 MLC. In the MLC control system view, right and left MLC bank is termed as Y1 and Y2 respectively. MLC is numbered from 1 until 80.

MLC 1 is the outermost MLC in which located at the positive Cartesian coordinate from the MLC control view. The leaves are 0.5 cm in width and are also capable of producing a 40 x 40 cm² maximum field size. The maximum manufacture's specified MLC speed of the system is 6.5 cm/s.

An MLC position feedback mechanism are implemented in the system to validate the accuracy of the MLC movement to the assign position. Varian Millennium applied motor current feedback mechanism on the MLC system to record the MLC position during the delivery. It relies on the feedback of the counts of the motor rotation that moves the MLC in a linear direction. Elekta Agility implemented optical tracking for its MLC position feedback mechanism. The positions are tracked in real-time by a camera system. These feedback mechanisms will be discussed more in Section 1.5.

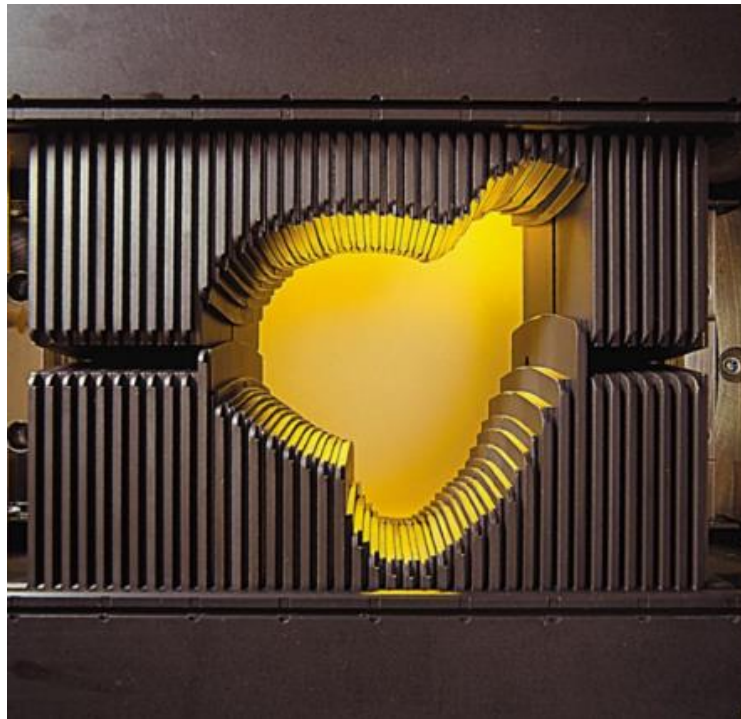


Figure 1.5: Photograph of the multileaf collimator (figure from www.newsroom.varian.com)

The improvement of the beam shaping technique by the application of the MLC ensures an efficient delivery of complex beam during radiotherapy treatment. These advancements allow efficient delivery of advanced radiotherapy treatment techniques such as Intensity Modulated Radiation Therapy (IMRT) and Volumetric Modulated Arc Therapy (VMAT). Both techniques deliver a highly conformal beam to the target volume with the use of the MLC.

Table 1: Mechanical characteristic of Varian Millennium and Elekta Agility MLC system

MLC technical characteristic	Varian Millennium	Elekta Agility
Number of MLC	120	160
Arrangement of MLC	60 pairs	80 pairs
Leaf width	1.0 cm (20 pairs of outer leaf) 0.5 cm (40 pairs of middle leaf)	0.5 cm for all 80 pairs of leaf
Maximum field size	40 x 40 cm ²	40 x 40 cm ²
Maximum MLC speed	2.5 cm/s	6.5 cm/s
MLC positioning feedback	Motor current	Optical tracking

1.3 Dynamic MLC based radiotherapy treatment

The MLC position sequencing algorithm in the treatment planning system (TPS) will create an appropriate MLC sequence when an optimised dose is achieved during planning. The sequence is generated by the TPS computer. The sequence consists of multiple segments of beam shape. The summation of the segments give a delivered fluence that is close to the optimised fluence [7]. These sets of MLC sequence can be delivered in several techniques. Intensity Modulated Radiation Therapy (IMRT) and Volumetric Modulated Arc Therapy (VMAT) are the recent techniques in radiotherapy

that utilise dynamic movement of the MLC. Both techniques modulate the radiation dose to the target by varying the intensity across different parts of target area.

1.3.1 Intensity Modulated Radiation Therapy (IMRT)

IMRT is a radiotherapy technique where the beam is modulated at a static gantry angle whereas the MLC moves dynamically during the exposure. There are two IMRT techniques that are used clinically. They are step-and-shoot or static MLC (sMLC) and the dynamic MLC (dMLC) methods.

In sMLC method, the modulated intensity is achieved by multiple static MLC segments as shown in Figure 1.6(a) [8]. MLC will only move to the prescribed position to form an irregular static field shape while the treatment beam is off [9]. The MLCs will stay at rest when the beam is delivered before it moves again to create the next segment field shape. For each static segment, the shape and prescribed monitor unit are distinct from each other. The static field is easy to verify and requires less complex quality assurance techniques because the MLC is static during treatment delivery and other factors such as the MLC speed has no effect on the accuracy [10]. Despite that sMLC requires longer treatment time as there is a beam hold-off time for the MLC to move between each segment.

The dMLC method is more complex to sMLC. The dose is delivered with continuous movement of the MLC during beam irradiation. The beam shape could be similar to the sMLC shape during the dynamic delivery as shown in Figure 1.6(b) but the MLCs are continuously changing the shape without any beam hold-off in between. The dMLC beam requires more monitor unit (MU) and wider range of MLC speed to deliver a more complex intensity pattern. Thus, the complexity of the dMLC technique is higher compared to sMLC.

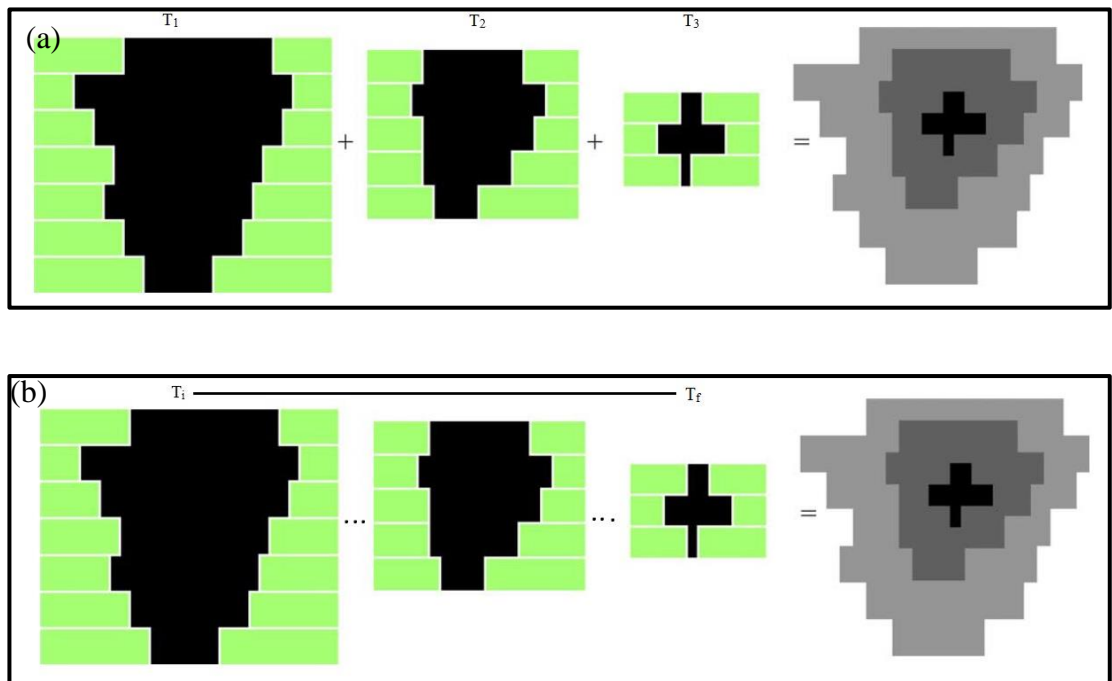


Figure 1.6: The sMLC (a) and the dMLC (b) field shape segment delivery (in colour) and the resulted fluence map (in grayscale) [8].

VMAT is a more complex radiotherapy technique than IMRT. The method is an extension to dMLC techniques to deliver IMRT. VMAT employs continuous MLC movement during irradiation whilst the gantry head are arcing around the patient. It involves variable dose rates and gantry speed to efficiently produce a highly conformal dose distribution [11]. VMAT is more efficient compared to IMRT as the beam is delivered continuously during the treatment. Due to the complex movement of the MLC and gantry, the complexity of the radiation delivery increases. The accuracy of the gantry angle and speed also need to be verified, in addition to the MLC components.

1.4 Quality assurance of IMRT and VMAT using clinical detectors

Advanced radiotherapy treatments are prone to delivery errors due to complex nature of the beam shaping. Patient specific quality assurance (QA) is an essential process in radiotherapy. It is performed to ensure the linac is able to deliver treatment plan as prescribed in the IMRT or VMAT plan. Dosimetric and mechanical aspect of the treatment plan should be assessed for each patient treatment plan before the treatment is delivered to the patient. The accuracy of the plan transferred to the linac, particularly the MLC sequence file, are verified during QA. During the QA procedure, the movement of delivery parameters such as the MLC, gantry head, and collimator will be verified to be moving correctly within the tolerance value. Dosimetric QA of the treatment plan is performed by comparing the dose delivered to a dosimeter with the dose calculated by the TPS for the same geometry [7]. The conventional method of performing patient specific QA using clinical dosimetry is by using film [12,13]. However, film measurement involves difficult calibration of the film and not preferable for patient specific dosimetry. In studies by Marrazzo *et al.*, an accurate calibration curve of the film is needed prior to dose analysis of clinical plan measured using a film [12]. The calibration factor ensures accurate conversion of the pixel values read out from the film to the dose value. Errors may be introduced if the calibration process is not performed accurately. Film also provides the dose distribution of the whole beam exposure on a two-dimensional (2D) plane.

Another measurement method of patient specific QA is by using 2D array detector. The advantage of using 2D array detector over film measurement is that it provides immediate results after beam delivery. The 2D array detector is placed in a phantom during measurement and the dose measured is compared with the prescribed dose. Letourneau *et al.* evaluated a type of 2D array called MapCheck for its feasibility

to be used in IMRT QA [14]. They conducted the study by verifying MapCheck's sensitivity to MLC errors. The clinical plans of head and neck (HN) were modified causing the MLC segments to contract and expand by 1 mm to 2 mm. MapCheck sensitivity to MLC error was evaluated by the variation of diode numbers that did not satisfy the dose and distance to agreement (DTA) analysis [15] with the unmodified prescribe plan. The same approach was performed by Hussein *et al.* using a different type of 2D array [16]. This group studied a 2D array ionisation chambers (PTW, Freiburg, Germany) that was combined with Octavius phantom for measurement. However, the results show none of the MLC error (1 mm, 2 mm and 5 mm) for head and neck (HN) cases of RapidArc plan were detected. Deliberated MLC error can only be detected with a stricter dose and DTA analysis passing criteria when it was from 1 mm to 2 mm for prostate and pelvic nodes RapidArc plan.

Recent studies also discussed patient specific QA measurement using electronic portal imaging device (EPID). The portal images of the beam captured using the EPID are sent to the TPS for dose recalculation. Defoor *et al.* performed such method. Cine (continuous) images of delivered beam were converted to an opening density matrix which resemble the fluence incident. TPS reads the matrix and performed dose recalculation [17]. Reconstructed dose from the EPID images shows mean deviation of 1.2% from planned distribution. There are other studies that compare processed images from EPID with portal dose predicted from TPS [18,19] that used dose reconstruction approach in the absence of patient or phantom per beam at the position of the EPID. Each study used different types of EPID and thus involves different image processing techniques. The method also does not provide any information regarding the performance of the individual MLC during treatment. Absolute MLC position from EPID images can only be acquired with the use of image

processing algorithm such as field edge detection [20,21]. Due to the slow EPID imaging speed, the sensitivity of EPID to MLC position error are low, and difficult to be detected. Bawazeer et al investigated this by introducing systematic error to IMRT plan [22]. The error causes larger leaf gap and shifted field to the original plan. High pass rates of gamma analysis show that EPID was unable to detect error as small as 1 mm. Moreover, for a large field in head and neck plan, some of the beam extended outside the detector area, resulting in missing data.

1.5 Real-time tracking data of linac parameters

In Section 1.4, the drawbacks of measurement based QA using dosimeters have been discussed. Treatment delivery information particularly the MLC positions are indirectly accessible from EPID and 2D array measurement. Hence the study motivates to evaluate the potential of real-time tracking data as part of patient specific verification of IMRT plan. Real-time tracking of the treatment parameters data is a mechanism that is available in a linac that allows verification MLC positions at certain sampling rate. The output of the tracking is stored as a log file which can be assessed for analysis. Varian linac uses different mechanism for real-time tracking compared to Elekta linac.

1.5.1 Varian linac

Varian linac uses motor current feedback for its real-time tracking mechanism. Each MLC is driven by a motor that is attached to an encoder. The encoder will channel out signal pulses to determine the direction of the MLC movement. The distance travelled by MLC is computed by counting the number of pulses, with each pulse containing four counts. A decoder will then decipher the information of the encoder pulses for each motor. It calculates how far each motor has rotated hence the distance travelled

by the leaves. This information is used to report the tracked position of each leaf to a resolution of 100 nm [23].

The information of the parameters is tracked every 50 ms. Values tracked are saved in a log file. In this study, we will refer the log file as Varian Log File (VLF). The planned treatment parameters are also recorded in the VLF during delivery. The planned MLC positions, fractional MU, jaw positions and gantry angle are interpolated linearly from the prescription received from the TPS [24,25]. In step-and-shoot IMRT delivery, linac beam state indicates the setup phase (step) and the delivery phase (shoot) for each segment. During the setup phase in which the MLC and gantry head are moving, the beam pause or beam hold-off is triggered, where the radiation is not delivered [26]. In addition to that, the beam hold-off pause is also triggered when the deviations between the tracked movement of delivery parameters and the prescription exceeds tolerance value. The beam is resumed when the parameters arrived at the prescribed positions.

The use of tracking data from VLF has been validated by a few studies. Li *et al.* experimentally measured the output of small MU segment of a simple-geometry pattern delivered by step-and-shoot mode [27]. Fractional MU from VLF were summed up for each static pattern and compared to the intensity detected by 2D diode array. The group found the deviation between the values from 2D array and VLF is within 2%. Zeidan *et al.* tracked MLC position using a fast video-based EPID for step-and-shoot IMRT delivery [28]. Images of the MLC collimations and the resulted fluence capture by EPID were compared to the information extracted from VLF. The results are within 5% agreement. The study characterised that VLF detected the undelivered segments and unplanned MLC movement during the delivery which were also detected by the EPID. The tracked MLC position from the VLF was also verified

using EPID image by Fuangrod *et al.* [21]. The captured EPID image is processed using edge detection that gives the information of the MLC position. The extracted positions were compared to the MLC position from VLF and the deviation of 0.2 mm to 1.4 mm were found. Kerns *et al.* performed mechanical analysis of IMRT clinical plan using VLF. The study reviewed thousands of VLF to determine typical RMS errors from Varian linac and the contributing factors of the errors. They have found that the mean and maximum MLC speed will affect the error significantly. These finding might not be accessible by verification measurement using dosimeters. The published studies in the literature shows an established use of VLF for tracking MLC position. The aim of this study is to develop an algorithm based on these literatures to analyse VLF. It is fundamental to the analysis of Elekta's log file. Elekta log file will be discussed in Section 1.5.2.

Information of IMRT delivery such as beam state, gantry angle and dose fraction are also utilised for verification of IMRT. All parameters in the VLF file are used as input for dose reconstruction of IMRT delivery [26,29,30]. The extracted MLC position back can be sent to the TPS for dose recalculation. The recalculated dose map from VLF were than compared to TPS dose. Dinesh *et al.* and Ortega *et al.* performed such method and found deviation of 4% and 1% respectively from the comparison. The capability of VLF to provide delivered treatment parameters for IMRT plan verification resulted in the development of automated software for data extraction and analysis of IMRT plan verification [31]. Analysis performed includes statistic of MLC deviation and comparison of the reconstructed fluence map.

1.5.2 Elekta linac

MLC tracking in Elekta linac is performed by optical tracking mechanism. Each MLC in the Agility system has an optically reflective marker on top of the leaf. Reflection of fluorescence light from the markers will be detected through a series of mirrors to a charge coupled device camera as illustrated in Figure 1.7. The camera is interfaced to a control computer that will record the MLC positions [32]. The tracked data is accessible through service graphing tool, a function on linac control computer that will record the tracked data at every 0.25 s. The tracked data are saved in log file that is retrievable from the control computer. In this study, we termed the log file as Elekta Log File (ELF).

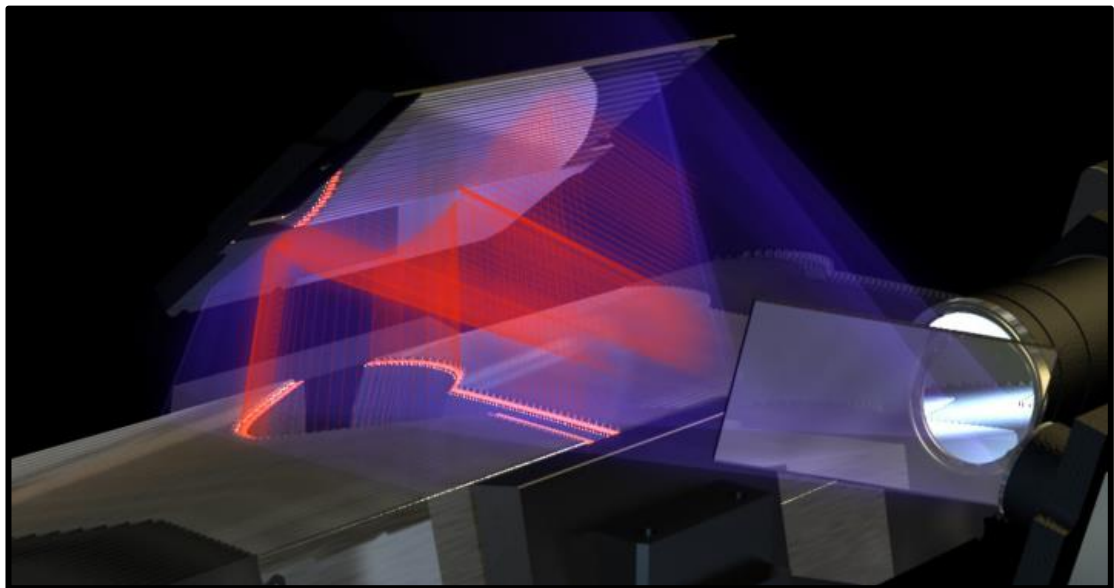


Figure 1.7: Optical tracking mechanism for Elekta Agility [33].

The use of tracking data from ELF in treatment plan verification hasn't been established in the literature. Arumugam *et al.* developed a software tool to analyse a binary log file from the linac control system. It contained records of delivery parameter errors summarised for each control points after a treatment is delivered. The binary log file does not contain real-time MLC positions during treatment. Pasler *et al.*

investigated the application of tracking data in mechanical QA of Elekta linac. In the study, beam parameters of a simulated dynamic MLC movement beam were tracked in real-time while the dose distribution were measured by 2D array detector. Correlation between these two data were made by comparing the MLC error and the dosimetric deviation measured by the detector [34]. The results show a large MLC error does not necessarily induce large dosimetric deviation in the detector. ELF had also been used for monitoring delivery parameters during VMAT on MLCi systems [35,36]. MLCi is an older generation Elekta MLC system with 1 cm of MLC leaf width. However, these studies did not perform any characterisation of the tracking data file prior of their study. Unlike VLF, the file structure of ELF is not clearly defined by the manufacturer and poorly described in the literature. The ELF is retrieved from the service graphing tool on the linac controls system. The procedure of retrieving ELF from service graphing tool is also not discussed in literature, thus limiting its application in IMRT QA.

1.6 Purpose of study

The main objective of the study is to investigate the utilisation of real-time tracking data for verification of dMLC based radiotherapy treatment. Real-time tracking data from two commercial linacs with different tracking mechanism were evaluated, hence giving three sub-objectives as follows:

- To verify IMRT treatment using real-time tracking data from Varian linac by analysing the MLC error, the MLC speed and the fluence map generated.
- To determine the characteristics of linac parameters in real-time tracking data of Elekta linac for application in IMRT verification.
- To verify IMRT treatment using real-time tracking data from Elekta linac by analysing the MLC error, the MLC speed and the fluence map generated.

CHAPTER 2 MATERIALS AND METHODS

2.1 Varian Clinac iX

2.1.1 Varian Millennium 120 MLC and tracking system

The characteristics of the MLC and its tracking mechanism have been described in Section 1.22 and Section 1.5.1. The MLC of Varian linac system were tracked every 0.05 s by the motor current. The tracked real-time MLC positions and other treatment parameters data were saved in a log file called Varian log file (VLF) after treatment delivery.

During an IMRT delivery, the MLC control system delivers the beam according to the treatment parameters prescribed in the controls points [37]. A large deviation between the tracked and prescribed position will cause beam hold-off [38]. During this beam hold-off state, the radiation delivery is paused, and the MLC will catch up the planned value. VLF file stored tracking data only during beam delivery. Based on descriptions in the literatures, an algorithm was developed to analyse real-time tracking data in VLF. The founding in this section will provide the basic framework to develop an algorithm to characterise Elekta Log File.

2.1.2 Characterisation of real-time tracking data from Varian linac

2.1.2(a) Varian log file

VLF is an established tracking data that has been used either in verification of radiotherapy linac parameters or reconstruction of IMRT fluence. The characteristics of VLF tracking data have been described in Section 1.5.1. Despite the numerous published work of VLF in the literature, the description of the algorithm to extract VLF data is not available. Hence, this study omits the basic characterisation of VLF tracking data but focuses on development of algorithm to analyse VLF. It will be the

basis for the algorithm development for characterisation of ELF. Analysis of both VLF and ELF will also allow comparison between the performances of the two log file systems. In addition to that, the data structure obtained in this study will be compared to published studies, and the algorithms developed to analyse the data will be used to evaluate IMRT treatment from a Varian linac. This section will describe the structure of the VLF and the characteristic of the data recorded in the file, published in the literature.

VLF is a comma separated value (csv) file generated after the delivery of a radiotherapy treatment. For each MLC bank of the Varian linac, one file is produced. Figure 2.1 (a) shows the structure of a raw VLF and Figure 2.1 (b) shows the structure after the data rearranged in an excel file. The first six lines contain the header of the raw file that includes the VLF version and patient information. The information on the treatment delivery parameters are recorded every 0.05 s line-by-line beginning line seven for the whole treatment delivery. Each column represents different parameters. First 14 columns record the dose fraction, segment number, beam state, segment dose index, gantry rotation, collimator rotation and jaw position. Prescribed and tracked MLC position information starts from the 15th column [30].

The next process is conversion of MLC position value to millimetre. VLF logged the MLC positions located at 51 cm from the source. The positions are recorded in units of one-hundredth of millimetre (1/100 mm). Equation 1 was used to calculate the position of the MLC at the isocentre levels in millimetres (mm). The magnification factor is 1.966 (100/51) based on the relationship of the radiation source-to-MLC-isocentre distance [36, 37]. Dose fraction is recorded in nominal range of 0 (0% of total dose) to 25000 (100% of total dose). Gantry and collimator angle are in one-tenths of degree (1/10°) while the jaw is in millimetre (mm). Finally the algorithm calculates the MLC position error (MLC error), MLC speed and construct the fluence map for each delivery. These variables will be discussed in Section 2.1.3.

$$\text{MLC position (mm)} = \frac{\text{Raw position}}{100} \times 1.966 \quad \text{Eq 1}$$

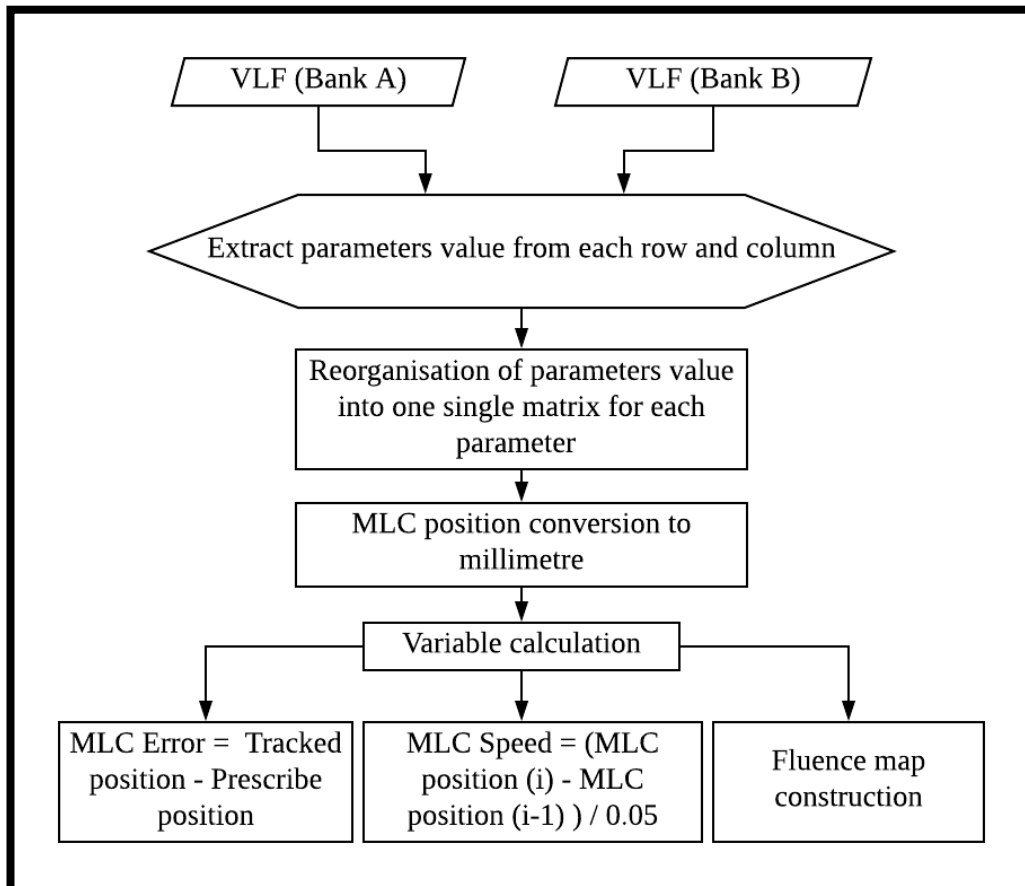


Figure 2.2: Flow chart of VLF file extraction algorithm

2.1.3 Application of real-time data tracking on clinical IMRT plan for treatment verification

The VLF file was used to evaluate performance of clinical IMRT treatment using algorithms developed in Section 2.1.2. Three head and neck (HN) IMRT cases delivered with dMLC technique at Loh Guan Lye Hospitals were analysed. All the plans deliver eight total beams at different gantry angle. Table 2.1 shows the gantry angles for each case. Treatment parameters from the VLF files were extracted using Matlab algorithm as mentioned in Section 2.1.2.

Table 2.1: Three IMRT cases delivered using Varian Clinac iX analyses in this study.

IMRT cases	Gantry angle (°)
HN 1	30, 80, 130, 180, 230, 290, 330
HN 2	80, 130, 180, 230, 280, 320, 350
HN 3	30, 80, 130, 180, 230, 280, 320

Analysis of the MLC position errors of the HN cases from the Varian linac was performed. MLC position errors (MLC error) and MLC speed were calculated using Equation 2 and Equation 3. The unit for each variable is in millimetre (mm) and centimetre per second (cm/s) respectively. The root mean square (RMS) that represents the average value of the MLC errors regardless the direction of the error was calculated using Equation 4 where N is the total number of tracked data. To study the effect of MLC speed and gantry angle on MLC error trends, the values were plotted as a function of MLC speed and gantry angle.

$$\text{MLC Error} = \text{MLC tracked position}(i) - \text{MLC prescribed position}(i) \quad \text{Eq 2}$$

$$\text{MLC Speed} = \frac{\text{MLC Position}(i) - \text{MLC Position}(i-1)}{0.05} \quad \text{Eq 3}$$

$$\text{RMS} = \sqrt{\frac{\sum \text{MLC Error}^2}{N}} \quad \text{Eq 4}$$

The dose distribution of the treatment was analysed through a construction of the fluence map. Prescribed and tracked fluence map were constructed from MLC positions and MU fractions data. An algorithm to construct the fluence map was developed using Matlab. Figure 2.3 shows a flow chart of the fluence map construction.

Firstly, an empty array of 40 cm x 40 cm that represents the maximum field size of the beam that can be produced by the MLC is constructed. The y-axis represents the field size along the width of each MLC. 20 outer MLC with 1.0 cm width produce 20 cm area at the upper and lower portion of the fluence map. The 40 middle MLC have width of 0.5 cm. It covers 20 cm middle area of the map. The x-axis of the map represents the MLC position in the field. Positional value of all MLC pairs was used to determine the exposed area at every 0.05 s.

Each pixel of the constructed empty array has initially zero value. The pixel value of the exposed area was incremented by the MU fraction value that was delivered at the respective time. MU fraction is calculated by finding the difference of MU between two consecutive times. Each VLF file corresponds to a treatment delivered at a single gantry angle. Fluence maps from each gantry angle were added together to construct the total fluence map for the whole IMRT treatment. The initial map is constructed in which one pixel represent 1.0 cm of the map area. It is then converted to mm to give higher resolution of the map.

Prescribed and tracked fluence map were compared to by calculating the difference between pixel values in the map. The constructed fluence map is normalised